Mössbauer Study of Hyperfine Fields and Isomer Shifts in the Fe-Rh Alloys*

G. SHIRANE, † C. W. CHEN, AND P. A. FLINN
Westinghouse Research Laboratories, Pittsburgh, Pennsylvania

AND

R. NATHANS

Brookhaven National Laboratory, Upton, New York

(Received 27 February 1963)

Hyperfine fields and isomer shifts of Fe^{57} in the Fe-Rh system have been investigated by the Mössbauer technique in the composition range between 0 and 52 at.% Rh. When the Rh concentration exceeds 20%, chemical ordering of CsCl type develops and two distinct hyperfine fields are observed, corresponding to Fe on Fe sites (FeI) and Fe on Rh sites (FeII). For example, $H_i(\mathrm{I})=277$ kOe and $H_i(\mathrm{II})=384$ kOe in an alloy containing 48% Rh. Neutron diffraction study of this alloy gave $\mu_{\mathrm{FeI}}=3.2\ \mu_B$, but no direct measurement is available for μ_{FeII}. It is suggested that FeII, which is surrounded by 8 Fe nearest neighbors, may have a smaller magnetic moment than FeI despite its higher hyperfine field. The alloy with 50% Rh transforms, on cooling, from ferromagnetic to antiferromagnetic at 65°C. At this phase transition the hyperfine field shows a discontinuous decrease of 14 kOe.

I. INTRODUCTION

AMONG the various alloy systems formed between iron and elements of the second or third transition series (partially filled 4*d* or 5*d* shells), the system iron-rhodium exhibits particularly interesting magnetic properties. Fallot[1] reported, in 1938, that the average magnetic moment of the alloys increases at first with the addition of rhodium to iron, and reaches a maximum at approximately 25 at. % rhodium, as shown in Fig.1. This implies that either the iron moment is increased considerably by alloying or the rhodium atoms carry a large magnetic moment in this system. A similar effect has been observed in the iron-platinum and iron-iridium systems; but only in the iron-rhodium system is the alpha phase field (bcc) sufficiently extensive so that a systematic investigation of the variation of the magnetic moments of the constituent atoms over a wide composition range is possible.

Unfortunately, the phase diagram of the iron-rhodium system is not well established. To clarify the discussion which follows, we offer a highly tentative version in Fig. 2. It is based largely on the work by Fallot,[1] with modifications and additions derived from observations made in the course of the present investigation. The addition of rhodium first lowers, and then raises the alpha-to-gamma transition temperature, producing a minimum near 20% rhodium. Also, at about this composition, ordering of the CsCl type appears—the phase designated as α' in the diagram. This phase extends to about 52% rhodium at about 900°C. The diagram is unknown above 1000°C, so that we do not know whether the iron-based gamma field is continuous with the terminal rhodium solid solution (also labeled gamma in our diagram) or not. The Curie point of the α and α' alloys is lowered by the addition of rhodium, reaching about 400°C at the phase boundary. An additional magnetic transformation occurs in alloys containing between about 48 and 52 at. % rhodium.[2–5] These alloys become antiferromagnetic, with the transition temperature *increasing* with increasing rhodium content, to somewhat above room temperature at the phase boundary. It has been clearly established that this is a first-order phase transition, from ferromagnetic to antiferromagnetic state, with a volume decrease of 1%.[3]

We have carried out a systematic investigation of this system by Mössbauer measurements using Fe^{57}. This technique gives two important quantities relevant to the magnetic properties of solids, namely, the hyperfine field, H_i, and the isomer shift, ΔE. Experimentally, the absorption spectra of Fe^{57} in a magnetically ordered state show six symmetrical peaks as a function of the relative velocity of source and absorber. The spacing of these peaks is proportional to the hyperfine field, and the shift of the center of this group from zero velocity is defined as the isomer shift.[6]

The relation between the hyperfine field and the magnetic moment in several iron-base alloys has already been investigated.[7–10] It is of considerable interest to

* This work was performed in part under the auspices of the U. S. Atomic Energy Commission.

† Present address: Brookhaven National Laboratory, Upton, New York.

[1] M. Fallot, Ann. Phys. (Paris) **10**, 291 (1938).

[2] M. Fallot and R. Hocart, Rev. Sci. **77**, 498 (1939).

[3] F. de Bergevin and L. Muldawer, Compt. Rend. **252**, 1347 (1961).

[4] L. Muldawer and F. de Bergevin, J. Chem. Phys. **35**, 1905 (1961).

[5] J. S. Kouvel and C. C. Hartelius, Suppl. J. Appl. Phys. **33**, 1343 (1962).

[6] L. R. Walker, G. K. Wertheim, and V. Jaccarino, Phys. Rev. Letters **6**, 98 (1961).

[7] C. E. Johnson, M. S. Ridout, T. E. Cranshaw, and P. E. Madsen, Phys. Rev. Letters **6**, 450 (1961).

[8] C. E. Johnston, M. S. Ridout, and T. E. Cranshaw, in *Proceedings of the International Conference on Mössbauer Effect, Paris, 1961* (John Wiley & Sons, Inc., New York, 1962), p. 142.

[9] P. A. Flinn and S. L. Ruby, Phys. Rev. **124**, 34 (1961).

[10] E. A. Friedman and W. J. Nicholson, Suppl. J. Appl. Phys. **33**, 1048 (1963).

investigate this relation in the Fe-Rh system, where a 4*d* transition element is involved and the magnetic properties exhibit the interesting features mentioned above. Of particular interest is the behavior of H_i through the ferromagnetic–antiferromagnetic transition, where a difference of the polarization of conduction electron in two states should reflect in a change of the hyperfine field.

As for the magnetic moment of Fe atoms in this system, direct neutron diffraction results are available, at present, only for alloys near 50% Rh. Using powder neutron diffraction data, Bertaut *et al.*[11] reported $\mu_{Fe}=3.04\,\mu_B$ and $\mu_{Rh}=0.62\,\mu_B$ for the 53% Rh alloy above 60°C, where this alloy is ferromagnetic. Recently, a single crystal of 48% Rh alloy was examined by the polarized-beam technique.[12] At room temperature where this alloy is ferromagnetic, the atomic momenta are

$$\mu_{Fe}=3.2\,\mu_B,\quad \mu_{Rh}=0.9\,\mu_B.$$

In this paper, we report the detailed investigation of the hyperfine fields and isomer shift over a wide concentration range. A part of the results was briefly reported recently[12] together with a preliminary account of the neutron diffraction study.

II. LATTICE CONSTANT AND MAGNETIC PROPERTIES

All alloys were prepared from high purity metals by levitation melting and the ingots were homogenized at 1200°C under vacuum at least one day. A few alloys were analyzed chemically, and the analyses agreed with the nominal compositions within 0.5 at. %. For each alloy, powder was produced by either grinding or filing. To secure the desired crystal structure (α phase) and to relieve residual stress and strain, the powder samples of the various alloys were subjected to prolonged annealing at different temperatures chosen originally on the basis of the diagram reported by Fallot[1] (see also Hansen[13]). After heat treatment, all samples were examined by x-ray diffraction, with iron $K\alpha$ radiation. The x-ray results are summarized in Table I and Fig. 3. Most heat treatments resulted in single phase alloys, but a few alloys were inadvertently annealed in two phase regions. These data were used in the construction of Fig. 2. Superlattice lines were observed for all alpha phase alloys containing 20% or more rhodium. An attempt was made to produce ordering of the Fe_3Al type in a 25% rhodium alloy, by cooling from 550 to 300°C at the rate of 1° C/h. No additional superlattice lines of the Fe_3Al type were observed. Attempts to suppress the CsCl ordering by quenching from just below the α-γ transformation temperature were unsuccessful. Some reduction in order was observed in the case of the 20% alloy; other compositions were unaffected.

In the course of the investigation, a martensitic transformation from γ to α was observed. This was used to obtain disordered alloys containing 20 and 25% rhodium. At 20% rhodium, the alloy quenched to room temperature from the γ field consists largely of martensitic disordered alpha; at 25%, further cooling to liquid-nitrogen temperature is required to convert the major part of the material. At 30% rhodium, no mar-

TABLE I. Lattice parameters and final heat treatment of Fe-Rh alloys. All of the alloys with bcc structure, except 10% Rh, are ordered in CsCl type.

At.% Rh	Unit Cell (±0.002 Å) α (bcc)	γ (fcc)	Heat Treatment
10	2.899		Furnace cool from 1000°C
20	2.929		12 days at 510°C
25	2.943		6 days at 570°C
25		3.671	Quenched from 1000°C
30	2.955		3 days at 500°C
30	2.942+2.970		3 days at 700°C
35	2.965		6 days at 600°C
35	2.958+2.978		3 days at 800°C
40	2.981		10 days at 1000°C
48	2.989		Furnace cool from 1000°C
49	2.993		Furnace cool from 1000°C
50	2.986		Furnace cool from 1000°C
51	2.987		Furnace cool from 1000°C
52	2.986	3.764	Furnace cool from 1000°C
60	2.986	3.763	Furnace cool from 1000°C
80		3.780	Furnace cool from 1000°C

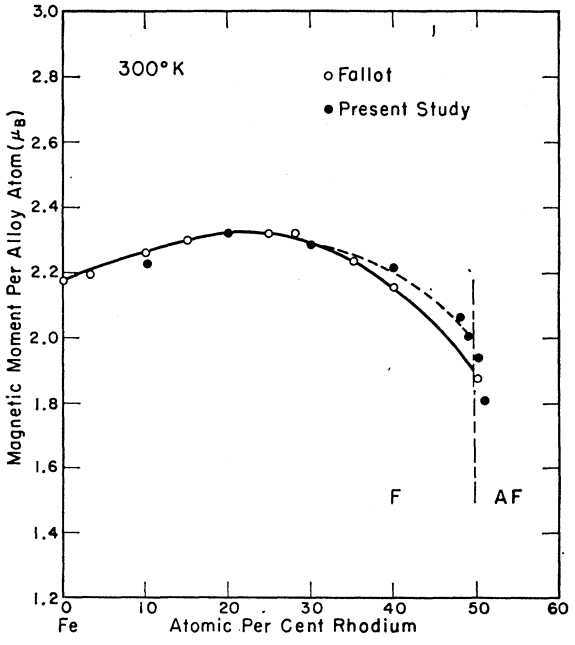

FIG. 1. Average atomic moment of Fe-Rh alloys at 300°K. The values in the antiferromagnetic phase were extrapolated from the data obtained in high-temperature ferromagnetic phase.

[11] E. F. Bertaut, A. Delapalme, F. Fowat, G. Roult, F. de Bergevin, and R. Pauthenet, Suppl. J. Appl. Phys. **33**, 1123 (1962).
[12] G. Shirane, C. W. Chen, P. A. Flinn, and R. Nathans, Suppl. J. Appl. Phys. **33**, 1044 (1963)
[13] M. Hansen, *Constitution of Binary Alloys* (McGraw-Hall Book Company, Inc., New York, 1958), p. 703.

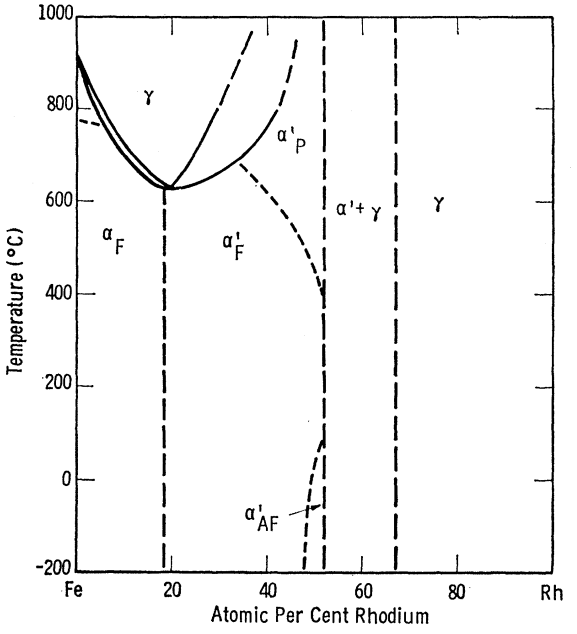

FIG. 2. Approximate phase diagram of the Fe-Rh system.

tensitic transformation of the quenched γ could be obtained, even by cooling to 4°K. The x-ray lines of the martensitic alpha showed the usual broadening characteristic of martensites, so that highly precise determination of the lattice parameter was not possible, and any possible small (<.003 A) change of lattice parameter was not detectable.

The lattice parameter shows a discontinuity between 49 and 50% Rh, where the room-temperature phase changes from ferromagnetic to antiferromagnetic. This result is consistent with the x-ray investigation of de Bergevin and Muldawer[3] on the alloy with 53% Rh. They obtained

$a=2.987$ Å at 15°C, antiferromagnetic,
$a=2.997$ Å at 65°C, ferromagnetic.

These two points are shown in Fig. 3 by solid circles.

With the preparative method we used, the α phase could not be obtained at room temperature beyond 51% Rh. This result is in agreement with the observation of Kouvel and Hartelius,[5] who reported a trace of γ phase in the 52% Rh composition with $a=2.99$A. Fallot and Hocart,[2] however, reported the magnetic data for the α phase up to 55% Rh.

Saturation magnetization was measured by a simple magnetic balance in a 6-in. magnet using a cylindrical sample, 2.7 mm long and 2.0 mm in diameter. The field gradient was calibrated with respect to ultra-pure nickel samples. The results of our measurements are shown in Fig. 1. In general, the agreement with the previous data is satisfactory. Some discrepancies were noted, however, in two sets of magnetic data for alloys near equiatomic composition. The transition temperature to the antiferromagnetic phase appears to be quite sensitive to composition as well as the state of chemical ordering. For 48% Rh, no transition was observed down to 4°K.

III. MÖSSBAUER MEASUREMENTS

Experimental

The Mössbauer spectra were measured with a constant velocity apparatus, using an electromagnetic drive and feedback control of velocity. The apparatus includes provision for direct and absolute measurement of velocity by measuring the time required for the traversal of a fixed and accurately known distance. The details of the apparatus are described elsewhere.[14]

The source was prepared by electroplating approximately 2 mC of Co^{57} onto a polished piece of chromium metal and diffusing it in by annealing approximately 30 min at 1100°C. Using this source and an absorber of iron foil 1 mil thick, we observed a linewidth (2Γ) of 0.4 mm/sec, a separation of the outermost peaks of 10.64±.03 mm/sec, and an isomer shift of 0.15±.02 mm/sec, in good agreement with previous measurements.[15,16]

The alloy specimens were prepared from iron-rhodium alloy powders of particle size less than 0.05 mm, sup-

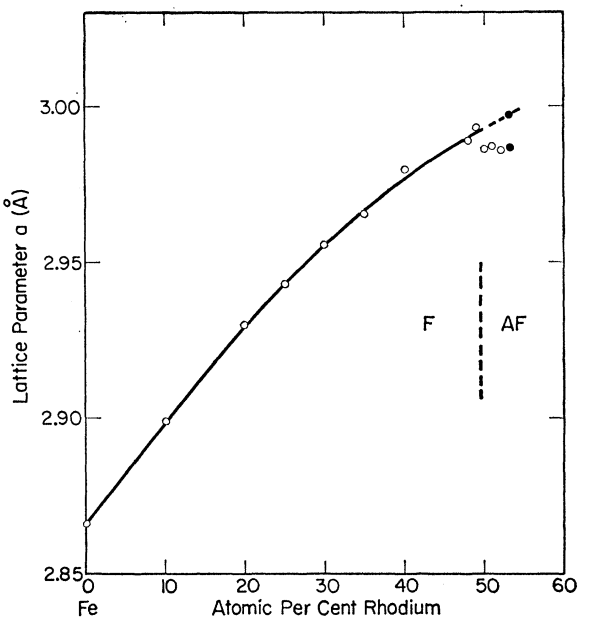

FIG. 3. Lattice parameter of Fe-Rh alloys. All alloys except 10% Rh are ordered in CsCl type. Solid circles shown at 53% Rh were given by de Bergevin and Muldawer (reference 3), the top one corresponds to ferromagnetic phase at 65°C.

[14] P. A. Flinn (to be published).
[15] S. S. Hanna, J. Heberle, C. Littlejohn, G. J. Perlow, R. S. Preston, and D. H. Vincent, Phys. Rev. Letters 4, 177 (1960).
[16] R. S. Preston, S. S. Hanna, and J. Heberle, Phys. Rev. 128, 2207 (1962).

ported on plastic, with the thickness of the powder layer adjusted to provide 10 to 20 mg/cm² of natural iron. The data are presented as percent absorption, relative to the total counting rate in the background. Each point represents $(2\text{–}6)\times10^5$ counts, so that the statistical uncertainty associated with each point is of the order of 0.2%.

Ferromagnetic Phase

The hyperfine fields and isomer shifts were measured as a function of composition as shown in Figs. 4 and 5.

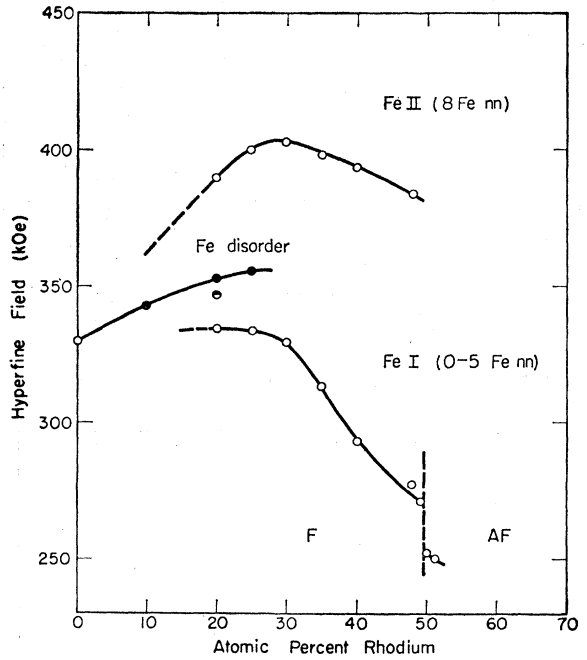

FIG. 4. The hyperfine fields at Fe^{57} in Fe-Rh alloys. The number of Fe nearest neighbors for FeI depends upon the composition as indicated in parentheses. The half-filled circle corresponding to 20% Rh is obtained for the partially ordered sample.

In the ordered phase with the Rh concentration 20–50%, two distinct hyperfine fields were observed. Here we define FeI as Fe atoms located on Fe sites in the ordered CsCl type structure and FeII on Rh sites. Thus, Rh sites are occupied at random by Rh and FeII. It should be emphasized here that all FeII atoms have identical nearest neighbors, namely, 8 FeI atoms, in the composition range between Fe and 50% Rh as long as the order is perfect. On the other hand, the number of Fe nearest neighbors of an FeI atom depends not only on the composition but also on the local distribution of FeII. In this respect, an FeI atom has a somewhat similar environment to an Fe atom in the disordered phase.

Typical absorption spectra are shown in Fig. 6 for the 25% Rh alloy, both ordered and disordered. The disordered phase pattern has the typical six peaks of

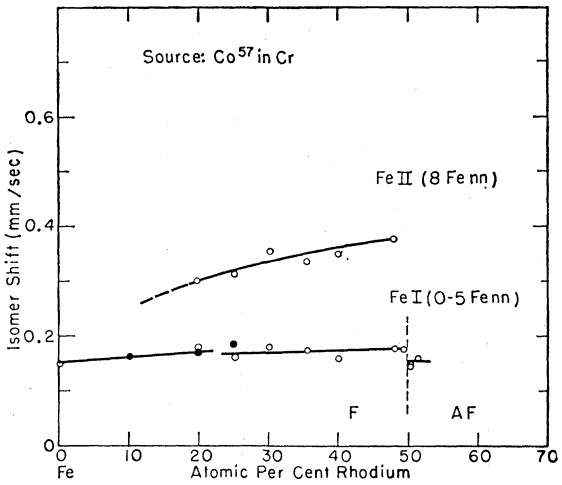

FIG. 5. Isomer shifts of Fe^{57} in Fe-Rh alloys. The source is Co^{57} in Cr and the positive velocity signifies a motion of source toward absorber.

a magnetic phase and, in addition, a single line at the center which arises from nonmagnetic γ phase. As mentioned above, the disordered α is obtained by a martensitic transformation of γ, and some retained γ is present. In the ordered phase, two sets of sextets were easily identified and indexed as shown in the insert. These are calculated using the two sets of outermost lines, which are clearly resolved, and the expected ratio of 2 FeI: 1 FeII for the perfectly ordered state.

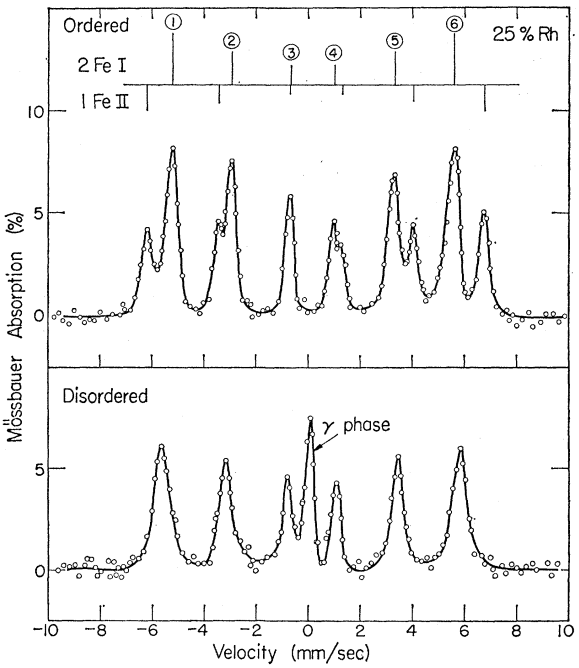

FIG. 6. Mössbauer spectra of ordered and disordered samples of 25% Rh. The disordered sample was prepared by a martensitic transformation and contains some γ (fcc) phase.

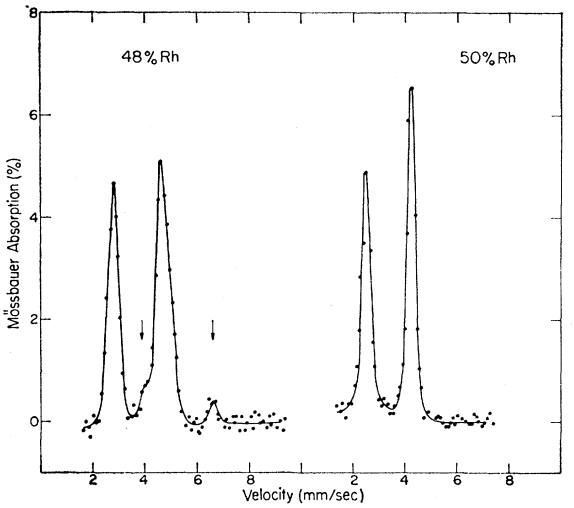

FIG. 7. Mössbauer spectra of 48 and 50% Rh. The absorptions due to FeII in 48% Rh are indicated by arrows.

From the relative intensities of two sets, there is little doubt that the larger hyperfine field corresponds to FeII.

This indexing is further confirmed by observing the change of relative intensities of the two sextets as a function of the rhodium concentration. The peaks assigned to FeII decrease with increasing Rh concentration, as expected, and disappear at 50% Rh (see Fig. 7). In 48% Rh, the FeII peaks are weak but definitely identifiable as shown by arrows.

An estimate of the relative numbers of FeII to FeI was made by comparing the areas under the absorption peaks. This process is more reliable than the one using the peak values of absorption, which may more readily be affected by line broadening. The estimate gave, for example, 0.54 for 25% Rh and 0.05 for 48% Rh. These are in satisfactory agreement with the expected value of 0.50 and 0.04, respectively, for the perfectly ordered alloys.

The peaks associated with Fe atoms in the disordered alloys, and with FeI in the ordered alloys are considerably broader than those for Fe in pure iron or FeII in the ordered alloys. This effect was first reported for Fe-Al alloys[9] and attributed to the variation in hyperfine field among iron atoms with different local enviroments. Similar results for Fe-Si alloys,[17] and additional work on Fe-Al alloys[10] have been reported since. In these studies only the effects of differences in nearest-neighbor environments were considered; recent work on Fe-Cr alloys,[18] which provide an exceptionally favorable situation for seeing the effect, indicate that second-neighbor effects also may play a fairly important role.

In the present investigation we did not attempt to decompose the peaks into contributions associated with various environments, but characterized each peak by a single parameter, the peak width, defined as the full width at half maximum height. In Fig. 8, we have plotted the widths of the innermost peaks (as triangles) and the outermost peaks (as circles) for the various types of iron sites. We note that the outermost peaks are broadened far more than the innermost, establishing that the broadening is, indeed, due primarily to a variation in hyperfine field and not in isomer shift with local environment. As expected, the broadening associated with the variation in hyperfine field disappears in the limits of pure iron and the perfectly ordered 50% Rh alloy. In each of these cases all Fe environments are identical. The broadening is greatest for the disordered 25% Rh alloy, where one would expect the largest variety of local environments. In the ordered alloys, the broadening associated with the FeI sites is much greater than that associated with the FeII sites. This also is to be expected. As pointed out above, the FeI atoms may have varying numbers of Fe nearest neighbors, but FeII atoms will have all Fe nearest neighbors in a perfectly ordered alloy. The small broadening which is observed for the FeII sites is probably associated with variations in second-neighbor environments.

The observed hyperfine field for the various types of iron sites is shown by solid lines in Fig. 9. It is clear that the hyperfine field at a given nucleus depends both on the bulk composition of the alloy and on the local environment of the atom. The dashed curves represent an attempt to estimate the variation of field with bulk composition for an iron atom with various numbers of iron neighbors. For simplicity, we ignore the effect of second neighbors. Only in one case, the 10% Rh alloy, did the effect of local environment appear as definite

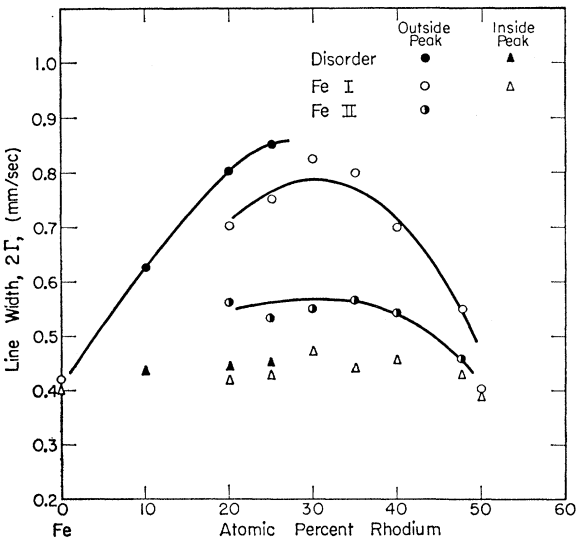

FIG. 8. Line width 2Γ of Mössbauer absorption spectra of Fe-Rh alloys.

[17] M. B. Stearns, Phys. Rev. **129**, 1136 (1963).
[18] P. A. Flinn (to be published).

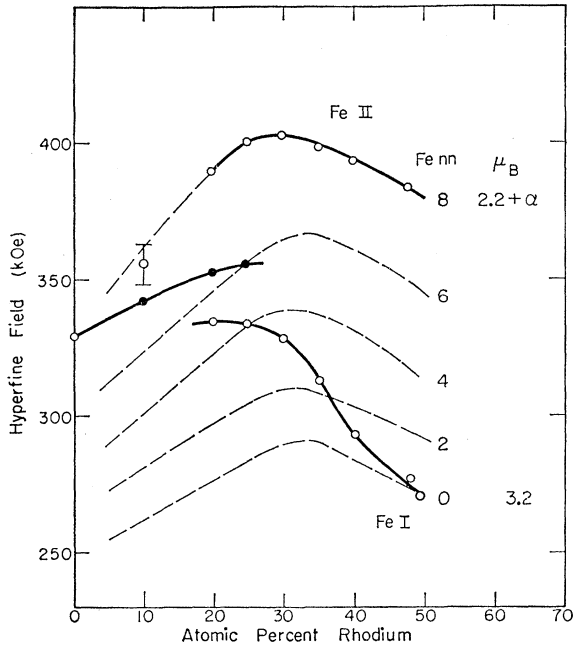

FIG. 9. Schematic diagram showing the hyperfine field distribution in Fe-Rh system. The point shown by an open circle for 10% Rh corresponds to a shoulder shown by an arrow in Fig. 10.

structure, rather than as broadening. In Fig. 10, we show the right hand outermost peak for the alloy, along with the corresponding peak for pure iron. There is a definite shoulder in the alloy peak which we ascribe to Fe atoms with all iron neighbors, while the main peak comes from those iron atoms with one or more rhodium neighbors. In a random alloy of this composition, approximately 43% of the iron atoms would have all iron neighbors. The area associated with the shoulder appears to be somewhat less than this, probably as a result of local order and second-neighbor effects. The hyperfine field obtained from this shoulder is plotted in Fig. 9 as the open circle with the large error flag. It is in reasonable agreement with the extrapolated curve for iron atoms with all iron neighbors.

Antiferromagnetic Phase

When the rhodium concentration reaches 50%, the room-temperature phase becomes antiferromagnetic, as shown by the magnetic measurement (Fig. 2). At this composition, the hyperfine field shows a discontinuous drop of 17 kOe, on going from the ferromagnetic to the antiferromagnetic state (Fig. 4).

This change is more directly demonstrated in the temperature dependence of the hyperfine field of 50% Rh, which becomes ferromagnetic at 338°K on heating (Fig. 11). The hyperfine field in the ferromagnetic phase follows quite closely the observed temperature dependence of the magnetization.[5] The change of the hyperfine field at the Néel temperature was estimated as 14 kOe.

The change of isomer shift at this phase transition is relatively small. It is estimated from Fig. 5 that it decreases from 0.18 mm/sec in the ferromagnetic phase to 0.15 mm/sec in the antiferromagnetic phase. The temperature dependence of the isomer shift of 50% Rh gives a similar result. In this measurement, what we actually measure is a "center shift," which is a sum of isomer shift and second-order Doppler effect. Since the latter changes almost linearly with temperature, a discontinuous change at the transition can easily be separated. This change was estimated as -0.03 ± 0.02 mm /sec on cooling, in good agreement with the change observed in Fig. 5.

γ Phase

This phase with face-centered cubic structure was only briefly investigated. Well defined γ phase was obtained only at two compositions. One is 25% Rh quenched from 1000°C and the other is 80% Rh, which is a single-phase γ at room temperature. The lattice constants of these two γ alloys are given in Table I.

The isomer shifts were determined at room temperature as

25% Rh 0.15 ± 0.02 mm/sec,

80% Rh 0.26 ± 0.02 mm/sec.

The values were determined using a Cr source which gives 0.15 ± 0.02 mm/sec for α Fe at room temperature. The linewidth, 2Γ, is 0.40 mm/sec for 25% Rh and 0.48 mm/sec for 80% Rh. Magnetic susceptibility measurement on 80% Rh revealed no magnetic transition down to 77°K.

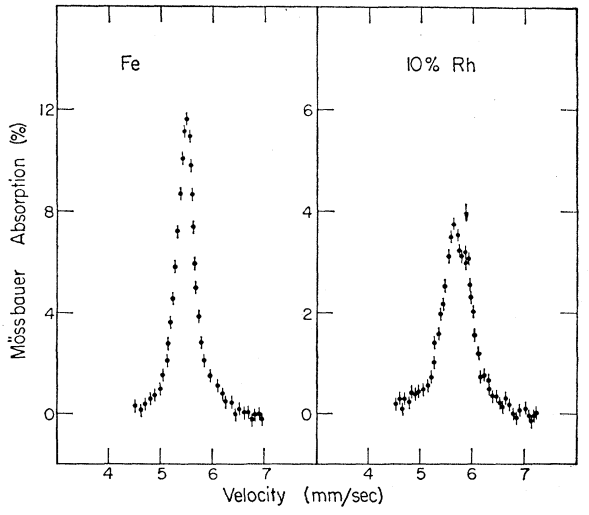

FIG. 10. Mössbauer absorption spectra of Fe and 10% Rh. The lines correspond to one of the outermost peaks of the sextet. The other peak, on the negative side, is almost symmetrical to the one shown here.

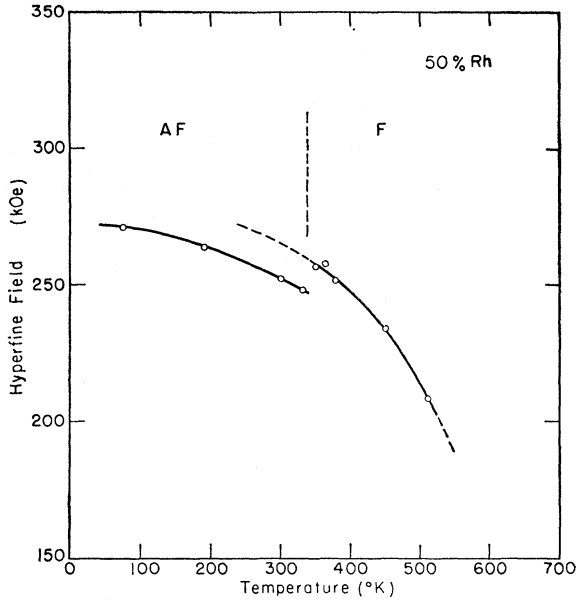

FIG. 11. Temperature dependence of the hyperfine field at Fe^{57} in $Fe_{0.50}Rh_{0.50}$. This alloy transforms from antiferromagnetic to ferromagnetic state at 338°K as shown by the broken line.

IV. DISCUSSION

In several studies of iron alloys,[7–9] the hyperfine fields at iron nuclei in various alloys were found to be roughly proportional to the magnetic moments of the iron atoms, with the ratio of about 150 kOe hyperfine field per Bohr magneton of moment. At least one important exception has already been reported, namely ordered $FeNi_3$.[7] In this case, the Fe moment measured by neutron diffraction[19] is 2.8 μ_B, while the value calculated from the hyperfine field using the above proportionality is only 1.8 μ_B.

In the Fe-Rh system, the FeI moment has been determined by neutron diffraction for the 48% Rh alloy to be 3.2 μ_B.[12] The hyperfine field for FeI at this composition is 277 kOe (Fig. 4), which by the proportionality quoted above would correspond to only 1.8 μ_B. It is clear that here also the proportionality relation fails completely. The FeI moment in this alloy is considerably larger than the moment of Fe in pure iron, while the hyperfine field is appreciably smaller. The situation is less clear for the FeII atoms, since we have no direct measure of their moments. Although the hyperfine field is larger for FeII (384 kOe) than for FeI, we need not assume that the moment is larger, since the proportionality rule has broken down. Moreover, unless the moments vary with composition in a most peculiar way, the average moment *vs* composition curve (Fig. 1) indicates that the moment of FeII atoms is somewhat less than that of FeI atoms.

It is interesting to note that, in contrast to the hyperfine field effects, the isomer shifts observed for the Fe atoms are not sensitive to the local environments. The shifts observed for FeI atoms are quite similar to that in pure iron and in the disordered alloys, despite the wide variations in nearest-neighbor environments. (See Fig. 5.) On the other hand, the shift observed for FeII atoms is quite different from that for pure iron, and varies markedly with composition, although the nearest-neighbor environment is virtually constant. If we assume that the interpretation of isomer shift given by Walker *et al.*[6] is at least roughly correct, these results imply that FeI atoms (iron atoms in proper sites) have an electronic configuration almost unaffected by alloying, while the FeII atoms (iron atoms in rhodium sites) acquire in some sense increased $3d$ or reduced $4s$ character.

We can roughly summarize the effects of rhodium on iron in this system as follows: rhodium neighbors increase the moment and reduce the hyperfine field of an iron atom, but apparently do not change the electronic configuration appreciably; iron atoms on rhodium sites in the ordered structure have a larger hyperfine field, probably a smaller moment, and an electronic configuration corresponding to an increase in d electron concentration. We offer a tentative interpretation of these results on the basis of the following assumptions. First, iron atoms in the pure metal have an electonic configuration which can be described roughly as consisting of seven rather tightly bound $3d$ electrons and one almost free electron, which we refer to loosely as $4s$ or as conduction electrons. Second, we assume that the conduction electrons are partially spin polarized antiparallel to the d electrons and contribute about -100 kOe to the total hyperfine field of about -330 kOe in pure iron. Third, we assume rhodium enters the lattice with roughly eight $4d$ electrons, as in the free atom, and contributes the one conduction electron. We can now attribute the effect of rhodium neighbors on the moment and hyperfine field of the iron atoms as due to a decrease in the polarization of the conduction electron spins. Since the rhodium atoms have much smaller moments than the iron atoms, the polarization of conduction electrons in their immediate neighborhood can be expected to be greatly reduced from its value in pure iron. This results in an increase in moment and decrease in magnitude of the hyperfine field at the neighboring iron. At the transition from the ferromagnetic to the antiferromagnetic state, a small further decrease in the magnitude of the hyperfine field occurs. We interpret this as due to the disappearance of the last of the spin polarization, since the conduction electrons may not be polarized in the antiferromagnetic state.

It is obvious now that a direct measurement of the magnetic moment of FeII is essential for the understanding of this system. This measurement, by neutron diffraction, is rather difficult in the alloys near 50% Rh. This is simply due to the fact that not enough FeII

[19] C. G. Shull and M. K. Wilkinson, Phys. Rev. **97**, 304 (1955).

atoms are present in the alloy to give the needed accuracy. We may recall that the moments are obtained from intensities of peaks, not from line position as is the case for the hyperfine fields. The study of the ordered alloy of 25% Rh can probably provide the needed information on the FeII moment. The task becomes considerably easier if one can obtain Fe_3Al-type ordering. As already mentioned, our effort to obtain this type of ordering was not successful. At present, we are attempting to obtain a single crystal of 25% Rh ordered in CsCl type.

ACKNOWLEDGMENTS

We are very grateful to W. J. Carr and D. E. Cox for many stimulating discussions, and should like to acknowledge the valuable assistance of M. Janocko and G. Gruber in various phases of the experiments.

PHYSICAL REVIEW VOLUME 131, NUMBER 1 1 JULY 1963

Field Dependence of the Direct-Process Spin-Lattice Relaxation Time in Rare-Earth Salts

D. HUBER*
Harvard University, Cambridge, Massachusetts
(Received 29 November 1962)

The field dependence of the direct-process spin-lattice relaxation time for rare-earth salts having $g_\perp=0$ is computed taking into account dipolar coupling between the spins. Comparison is made with the corresponding relaxation time calculated in a modified effective-field approximation, and the presence of terms not found in the modified effective-field formula is noted. Conditions that must obtain for the effective-field approximation to be valid are discussed, and a numerical evaluation of the relaxation time for dysprosium ethyl sulfate is given. Extension of the calculation to salts not having $g_\perp=0$ is also considered.

I. INTRODUCTION

THE purpose of this note is to extend to one-phonon processes the calculation of the field dependence of the spin-lattice relaxation time. Because of the complexity of the equations we will present explicit expressions for the relaxation time only for those salts having $g_\perp=0$. The formalism used will be that of Van Vleck,[1] Gorter,[2] and Hebel and Slichter,[3] while the notation will be similar to that of Orbach,[4] who computed the field dependence of the two-phonon process. Although we restrict our treatment to spin-lattice relaxation in rare earth salts, the theory is also applicable to the iron group salts, with certain provisos that are discussed in *O*I. Mention must also be made of the work of Bolger[5] who has considered the field dependence of the spin-lattice relaxation time from a somewhat different point of view.

* This work is partially supported by the National Science Foundation, and the Advanced Research Projects Agency, Department of Defense.
[1] J. H. Van Vleck, Phys. Rev. **57**, 426 (1940).
[2] C. J. Gorter, *Paramagnetic Relaxation* (Elsevier Publishing Company, Inc., Amsterdam, 1947).
[3] L. C. Hebel and C. P. Slichter, Phys. Rev. **113**, 1504 (1959).
[4] R. Orbach, Proc. Roy. Soc. (London) **A264**, 458 (1961); **A264**, 485 (1961). Hereafter referred to as *O*I and *O*II.
[5] B. Bolger, thesis, Leiden, 1959 (unpublished).

II. DERIVATION OF THE GENERAL FORMULA FOR THE RELAXATION TIME

We begin with the general expression for the relaxation time,[3] T_1,

$$\frac{1}{T_1}=\frac{1}{2}\frac{\sum_{\alpha,\beta}(E_\alpha-E_\beta)^2W_{\alpha\beta}}{\sum_\alpha E_\alpha^2}, \tag{1}$$

where $W_{\alpha\beta}$ is the net relaxation rate between the levels α and β, which have energies E_α and E_β. The spin-lattice relaxation process takes place via the orbit-lattice interaction as discussed in detail in *O*I. We restrict our attention to Kramers salts, the extension to non-Kramers salts being straightforward. In the case of Kramers salts the states $|\alpha\rangle$ and $|\beta\rangle$ form a time-conjugate doublet in the absence of perturbations. A perturbation is, therefore, introduced to remove the degeneracy of the ground state and to couple in the excited states so that the relaxation process might take place. In our problem the perturbation V' is the sum of the dipolar and Zeeman interactions. That is,

$$V'=V_{\rm dip}+V_z, \tag{2}$$

where

$$V_z=\sum_j \beta\Lambda\mathbf{H}\cdot\mathbf{J}^{(j)}, \tag{3}$$

and

$$V_{\rm dip}=\beta^2\Lambda^2\sum_{(j,k)}\frac{1}{r_{jk}^3}(A+B+C+D+E+F), \tag{4}$$